FY-2015 Methyl Iodide Deep-Bed Adsorption Test Report

Fuel Cycle Technology

Prepared for
U.S. Department of Energy
Material Recovery and Waste Form Development Campaign

Nick Soelberg
Tony Watson
Idaho National Laboratory
September 30, 2015

FCRD-MRWFD-2015-000267
INL/EXT-15-36817

ACKNOWLEDGEMENTS

We acknowledge others who helped guide or perform methyl iodide adsorption testing this year. Jack Law of the Idaho National Laboratory (INL) and Bob Jubin of the Oak Ridge National Laboratory provided programmatic and technical direction. Cathy Rae in the INL Chemistry and Radiation Measurement Department performed gas chromatography with mass spectrometry analyses. Duane Ball in the INL Chemistry and Radiation Measurement Department performed iodine sample analyses. Amy Welty of the INL Aqueous Separations and Radiochemistry Department assisted with data reduction.

This page blank

SUMMARY

Nuclear fission produces fission and activation products, including iodine-129, which could evolve into used fuel reprocessing facility off-gas systems, and require off-gas control to limit air emissions to levels within acceptable emission limits.

Deep-bed methyl iodide adsorption testing has continued in Fiscal Year 2015 according to a multi-laboratory methyl iodide adsorption test plan. Updates to the deep-bed test system have also been performed to enable the inclusion of evaporated HNO_3 and increased NO_2 concentrations in future tests. This report summarizes the results of these activities.

Test results showed that iodine adsorption from gaseous methyl iodide using reduced silver zeolite (AgZ) resulted in initial iodine decontamination factors (DFs, ratios of uncontrolled and controlled total iodine levels) under 1,000 for the conditions of the long-duration test performed this year (45 ppm CH_3I, 1,000 ppm each NO and NO_2, very low H_2O levels [3 ppm] in balance air). The mass transfer zone depth exceeded the cumulative 5-inch depth of 4 bed segments, which is deeper than the 2-4 inch depth estimated for the mass transfer zone for adsorbing I_2 using AgZ in prior deep-bed tests.

The maximum iodine adsorption capacity for the AgZ under the conditions of this test was 6.2% (6.2 g adsorbed I per 100 g sorbent). The maximum Ag utilization was 51%.

Additional deep-bed testing and analyses are recommended to (a) expand the database for methyl iodide adsorption and (b) provide more data for evaluating organic iodide reactions and reaction byproducts for different potential adsorption conditions.

This page blank

TABLE OF CONTENTS

LIST OF FIGURES

LIST OF TABLES

ACRONYMS AND ABBREVIATIONS

AgZ	silver zeolite
DF	decontamination factors
DL	detection limit
DOE	Department of Energy
DOG	dissolver off-gas
ECD	electron capture detector
EDS	energy dispersive spectroscopy
FCT	Fuel Cycle Technology
FID	flame ionization detector
FP	fission product
FY	fiscal year
GC	gas chromatograph
GCMS	gas chromatography with mass spectrometry
ICPMS	inductively coupled plasma mass spectrometry
INL	Idaho National Laboratory
ORNL	Oak Ridge National Laboratory
SEM	scanning electron microscopy
SPME	solid-phase micro-extraction

This page blank

1. INTRODUCTION

Nuclear fission results in the production of fission products (FPs) and activation products. If used nuclear fuel is reprocessed, some of those FPs and activation products, including iodine-129, could evolve into the process off-gas systems, and would likely require off-gas control to limit air emissions to levels within acceptable emission limits.

The Department of Energy (DOE) Fuel Cycle Technology (FCT) Program has supported research and development on iodine control and iodine waste forms for the past several years. The Offgas Sigma Team was formed in 2009 within the Separations and Waste Forms Campaign (now called the FCT Material Recovery & Waste Form Development Campaign) to establish a team of researchers from different DOE sites to focus on research and development for emissions control and waste forms for volatile radionuclides.

Capture efficiencies for I-129 may need to be high enough to achieve off-gas decontamination factors (DFs) of at least 3,000 (99.97% capture efficiency) to comply with applicable reprocessing facility regulatory requirements [Jubin 2012a]. Iodine control may need to be used on multiple reprocessing facility off-gas streams (such as the head end off-gas, dissolver off-gas, vessel off-gas, and waste treatment off-gas streams), because I-129 in the used fuel is likely to distribute at up to percent levels to different off-gas streams [Jubin 2013]. Iodine is known to exist in off-gas streams as diatomic I_2, and also react with other compounds in used fuel reprocessing streams including inorganic acids and organic species such as organic solvents or organic diluents used in actinide separations, or degradation products of those organic compounds, to form other iodine species including organic iodides [Bruffey 2015].

Research, demonstrations, and some reprocessing plant experience have indicated that diatomic iodine can be captured with efficiencies high enough to meet regulatory requirements [Soelberg 2013]. Research on the capture of organic iodides has also been performed, but to a lesser extent [Jubin 2012b, Soelberg 2015]. Several questions remain open regarding the capture of iodine bound in organic compounds.

A test plan identifies organic iodide data gaps and outlines a multi-year test program for advancing understanding and capabilities for capturing organic iodides on solid sorbents [Jubin 2012b]. This report summarizes the first phase of methyl iodide adsorption work performed according to this test plan using the deep-bed iodine adsorption test system at the Idaho National Laboratory (INL), performed during Fiscal Year (FY) 2013 and early FY-2014.

All work was performed in compliance with work control documentation that was updated in FY-2013 to ensure data quality, worker safety, environmental protection, and regulatory compliance during testing (INL 2014).

2. DEEP BED IODINE SORBENT TEST SYSTEM

Figure 2-1 shows a process diagram for the iodine test system. The test system consists of the following main components:

- Process gas supply and blending system, which supplies gases from gas cylinders, gas generators, and a humidifier
- Multiple sorbent bed system inside a heated oven
- Process gas bypass
- Inlet and bed segment outlet gas sampling system.

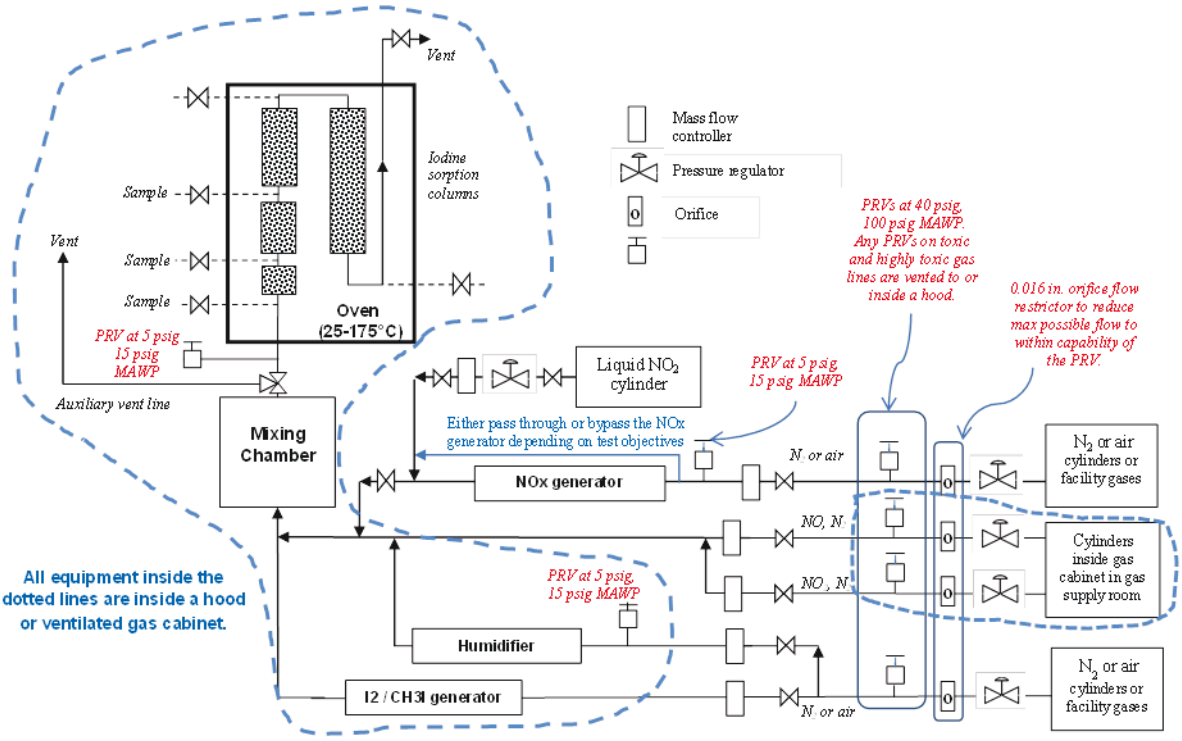

Figure 2-1. Deep-bed adsorption test system.

2.1 Process Gas Supply System

The process gas supply system consists of pressurized gas cylinders and gas generator systems that supply the gases that are blended together to make the gas mixture that is passed through the sorbent beds. These gases can include (depending on the test) pure air, nitrogen, NO_x, water vapor, diatomic iodine, and methyl iodide (as a surrogate for organic iodide). Air or N_2 can be supplied through mass flow controllers separately to the iodine and methyl iodide generators and the humidifier. NO and NO_2 gases, with balance N_2, are supplied from compressed gas cylinders through mass flow controllers. A New NO_2 generator system supplies higher NO_2 concentrations than can be provided from compressed gas. Gaseous HNO_3 is supplied by a new HNO_3 generator system.

Methyl iodide and iodine gases are provided using compressed gas cylinders, permeation tubes, or a fixed bed iodine generator. The choice of methyl iodide and iodine source depends on the flowrate needed to achieve the target concentration in the test gas mixture. For lower methyl iodide concentrations under about 1 ppm, compressed gas cylinders or a permeation tube system are used. For low iodine concentrations (under about 2 ppm) or for methyl iodide concentrations above about 1 ppm, the permeation tube system is used. For higher iodine concentrations above about 2 ppm, a fixed bed of iodine crystals interspersed in glass beads (which prevents iodine crystal agglomeration) is used.

The permeation tube system uses semi-permeable tubes that contain liquid methyl iodide (or solid iodine crystals) to emit a known flowrate of methyl iodide (or iodine) at a constant rate which is controlled by the operating temperature of the tube. The tubes (up to two), from VICI Metronics, are

placed inside a Dynacalibrator Model 190 constant temperature permeation tube system (Figure 2-2) also from VICI Metronics.

The gas flowrates and the generation rates of vaporized iodine, methyl iodide, and water are set to achieve the target gas composition and blended in a mixing chamber upstream of the sorbent beds. All process lines that contain vaporized iodine, methyl iodide, or water are electrically heat traced.

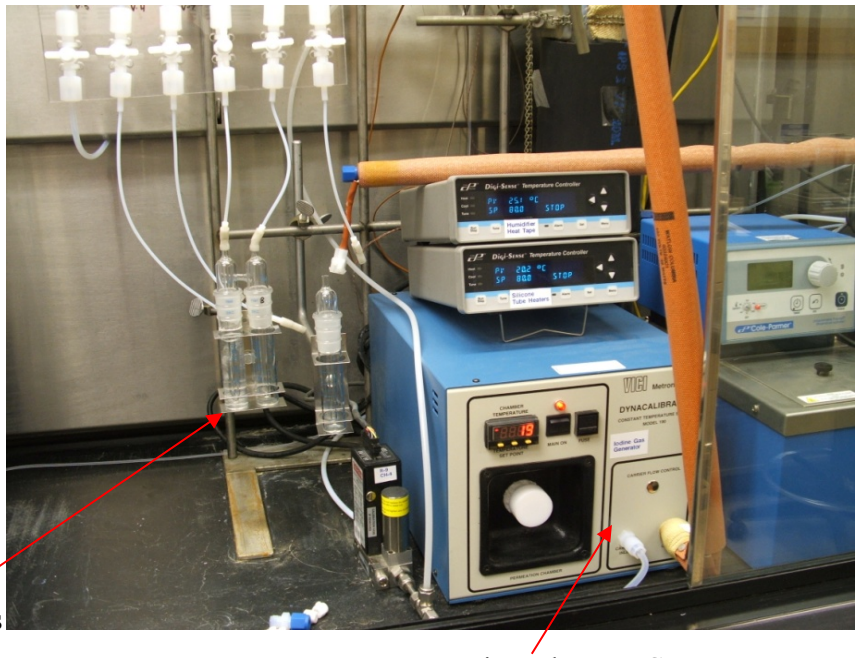

Figure 2-2. View of the iodine impingers and the permeation tube iodine or methyl iodide generator.

Humidified air is produced by passing air or nitrogen through a fritted glass bubbler submerged in a constant temperature water bath. A thermocouple in the headspace of the bubbler provides the temperature of the water-saturated gas. The concentration of water in the blended gas is controlled by adjusting the gas flowrate through the humidifier and the humidifier operating temperature.

2.2 ADDITION OF NO_2 AND HNO_3 GENERATOR SYSTEMS TO THE DEEP BED IODINE SORBENT TEST SYSTEM

For the recent Case Study (Law 2014) and based on results of dissolver off-gas testing by Birdwell 1991, benchmark total NO_x levels in the dissolver off-gas stream downstream of a recycling condenser have been estimated at 1 volume %, of which NO is 30% (3,000 ppm) and NO_2 is 70% (7,000 ppm) of the total NO_x. Deep-bed iodine adsorption testing has not yet included evaporated HNO_3, though there is a potential for evaporated HNO_3 in the dissolver off gas (DOG) downstream of the condenser.

The amount of NO_2 that can be provided in compressed gas cylinders is limited because higher NO_2 concentrations in N_2 are pressure-limited, and higher gas cylinder pressures have limited NO_2 concentrations. The maximum pressure in a 10,000 ppm NO2 compressed gas cylinder is about 330 psig, as compared to typical pressures in commercial compressed gas cylinders of about 2,000 psig. It is not practical or cost-effective to use compressed gas cylinders of NO_2 for long-duration deep-bed iodine

adsorption testing with NO_2 levels greater than about 1,000 ppm in gas streams at flowrates up to about 1 L/min.

During FY15 a gaseous NO_2 generator and a gaseous HNO_3 generator were each designed, procured, and successfully tested to enable higher concentrations of NO_2 as well as adding HNO_3 vapor to blended gas streams for the deep-bed iodine adsorption tests. Both these generator systems required design and operation to mitigate hazards and approval from INL safety and fire subject matter experts for updating work control documentation (INL 2015).

2.2.1 HNO_3 Generator

Acceptance criteria for the HNO_3 generator system were defined to be:

- Measurable and controllable HNO_3 flowrate.
- Complete evaporation of HNO_3 solution at the target flowrates.
- Avoid condensation after the HNO_3 solution is evaporated.
- Capable of blending gaseous HNO_3 with other test system gas flows – from the iodine or methyl iodide gas generators, NO/NO_2 supply systems, the humidifier, or dry air/N_2.

Two designs were initially considered. The first design was based on a heated vessel containing nitric acid solution. With a sweep gas (air or N_2) through the vessel and an azeotropic solution of HNO_3 (70 wt% HNO_3 in water), this design would be able to vaporize a constant ratio and amount of both water and HNO_3 into the sweep gas stream. The rate of evaporation would depend primarily on the heat input. This design would require a carefully controlled heat input, operation of the vessel at up to 121°C (at 1 atmosphere pressure), and a very accurate measurement of the evaporation rate. The evaporation rate would most accurately be measured using a load cell, but a load cell with the weight measuring capacity for the total mass of the vessel evaporation system (up to about 10 kg) would be barely sensitive enough to track the target evaporation rate over time (nominally up to 1.7 g/hr [1.2 ml/hr]).

The second design was considered and selected for testing and operation, because it required less sensitive heat input control and was more suited to tracking weight loss using a load cell. This design (Figures 2-3 and 2-4) provides a better method for the HNO_3 evaporation and flow control. It uses a syringe pump to supply measurable and controllable flowrates of HNO_3 solution to a commercial nebulizer inside a heated oven. Atomizing gas (air or N_2) atomizes and evaporates the HNO_3 solution as it enters the nebulizer. The nebulizer is constructed of glass, enabling the operator to see if the entire amount of HNO_3 is being evaporated. If it is not, then the operator can increase the oven temperature or increase the atomizing/evaporation gas flowrate.

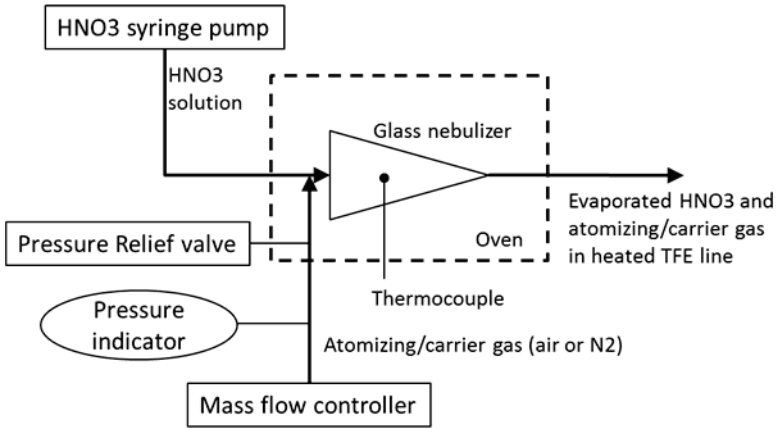

Figure 2-3. HNO_3 generator system schematic.

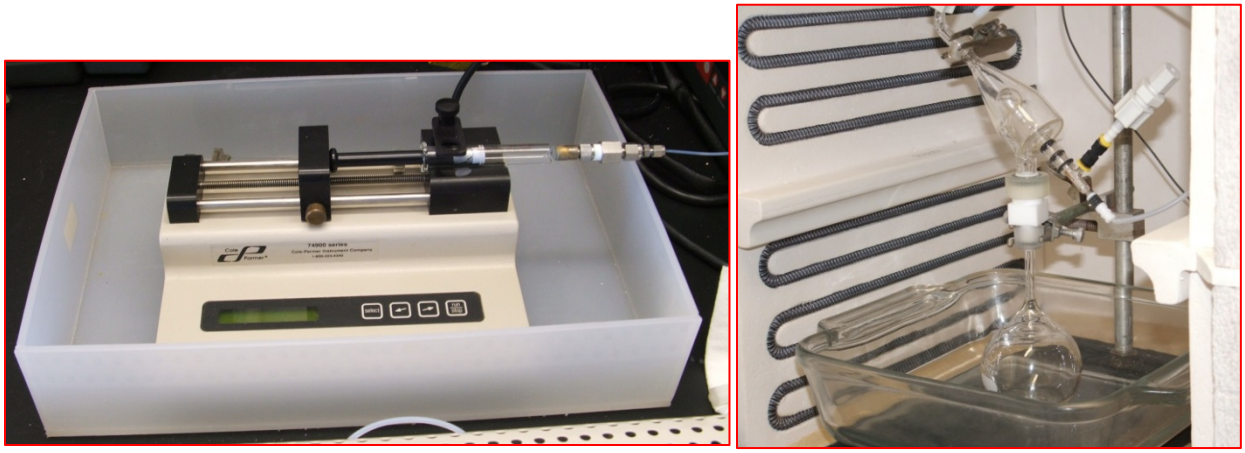

Figure 2-4. HNO_3 generator system syringe pump and nebulizer inside laboratory oven (not equally scaled).

The mixture of the evaporated HNO_3 solution and atomizing air passes through heated Teflon lines to be blended with the other gas flows to produce a mixed gas stream for iodine adsorption testing.

The HNO_3 evaporation system has been operated at different atomizing gas and HNO_3 flowrates to achieve total NO_x ($NO + NO_2 + HNO_3$) concentrations up to 37,000 ppm (3.7 volume %). Operating conditions for the HNO_3 evaporator system include:

- HNO_3 solution flowrates from 0.1 to 1.2 ml/hr. These small flowrates are adequate for providing the needed flowrates of gaseous HNO_3.
- Atomizing air flowrates from 200 to 800 ml/min.
- Oven temperatures from 40 to 100°C.
- Nebulizer temperatures up to 95°C.
- Nebulizer back-pressures from 2 to 11 psig.
- Heated line temperatures up to 150°C.
- Partitioning of NO_x gas evolved from the HNO_3 evaporation: NO_2 up to 110 ppmv, NO up to 13 ppm, HNO_3 up to 37,000 ppm (calculated by difference).

The impact of this evaporated HNO_3 gas on CH_3I stability was evaluated by blending a gas stream of CH_3I with the evaporated HNO_3 gas mixture, and measuring the concentrations of resultant CH_3I and combined iodine species that are soluble in 0.3 M NaOH (which includes HI and I_2). Table 2-1 shows that with no added CH_3I, the HI/I_2 was low, as it should be. With added CH_3I, a small amount, averaging 4.7%, of the iodine in the CH_3I was converted to HI/I_2.

Table 2-1. Conversion of iodine in CH_3I, exposed to evaporated HNO_3, to HI/I_2.

HNO_3 solution flowrate, ml/hr	Total NO_x concentration in the mixed gas, ppm	CH_3I concentration in the mixed gas, ppm	HI/I_2 concentration in the mixed gas, ppm	Conversion of iodine in the CH_3I to HI/I_2, %
0.3	2700	0	Average 0.034	---
1.1	9600	0		
1.1	9600	24-60	---	Average 4.7%

2.2.2 NO_2 Generator

The NO_2 generator evaporates liquid NO_2 into a gas for blending with the other gas streams that comprise the gas mixture for deep-bed iodine adsorption tests. The ability to use pure liquid NO_2 (which, at ambient temperature and in liquid form dimerizes to N_2O_4) has been developed by working with INL safety and fire subject matter experts. The work control procedures were updated to include and control the safe use of small amounts (nominally up to 1 lb) of liquid NO_2 (INL 2015).

Key to using liquid NO_2 as the source of gaseous NO_2 is, first, mild heating of the liquid NO_2 cylinder to not more than 50°C (the cylinder safety limit) to create sufficient pressure in the cylinder (Figure 2-5) and provide heat for vaporizing the N_2O_4 and the endothermic conversion of N_2O_4 to NO_2. Second, the conversion of gaseous N_2O_4 dimer to NO_2 should be assured by heating the gas stream to about 150°C if possible. At this temperature, the equilibrium constant for the conversion of N_2O_4 to NO_2 favors NO_2 (Figure 2-6) [http://chemed.chem.purdue.edu/demos/main_pages/21.1.html] and facilitates NO_2 flowrate monitoring and control.

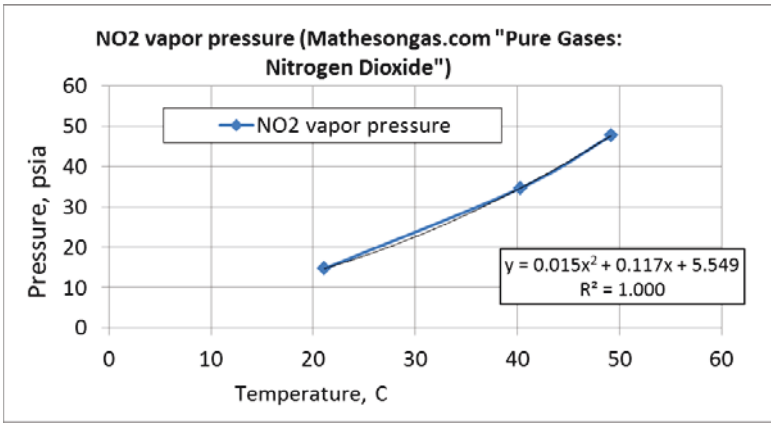

Figure 2-5. NO_2 vapor pressure.

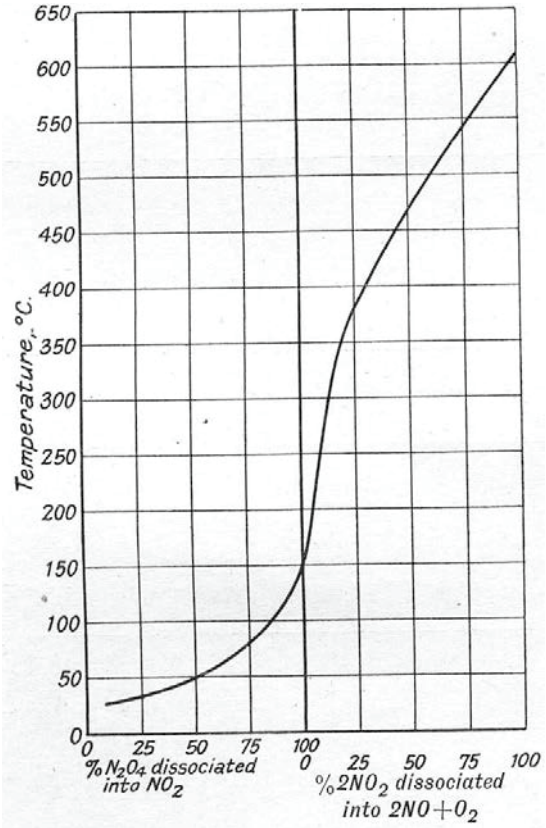

Figure 2-6. N_2O_4 and NO_2 dissociation equilibria (from Edmund 1928).

The NO_2 gas is promptly blended after flowrate control with the carrier gas (Figure 2-7) to lower the NO_2 concentration and prevent condensation. This blend of NO_2 and carrier gas is then mixed with the rest of the gas mixture to be used in deep-bed iodine adsorption testing.

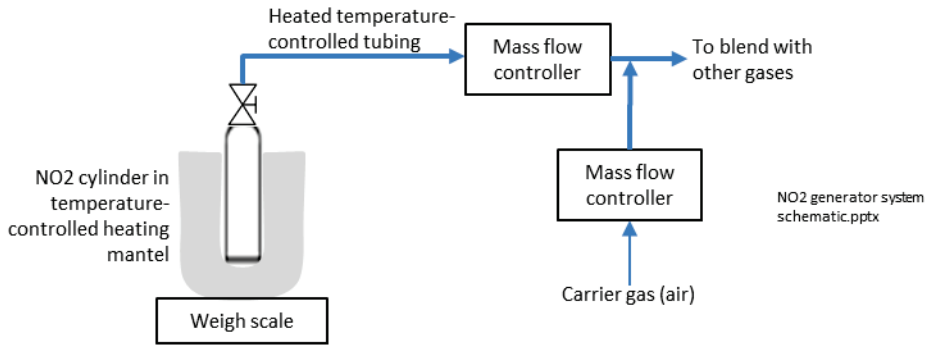

Figure 2-7. NO_2 generator system schematic.

2.3 Sorbent Bed Segments

Figures 2-8 and 2-9 show detail of the sorbent beds and how the sorbent beds are configured in a temperature-controlled oven. The current test design includes up to four sorbent bed segments. The sorbent bed segments are made of borosilicate glass. A glass frit at the bottom of each bed segment supports the granular AgZ sorbent.

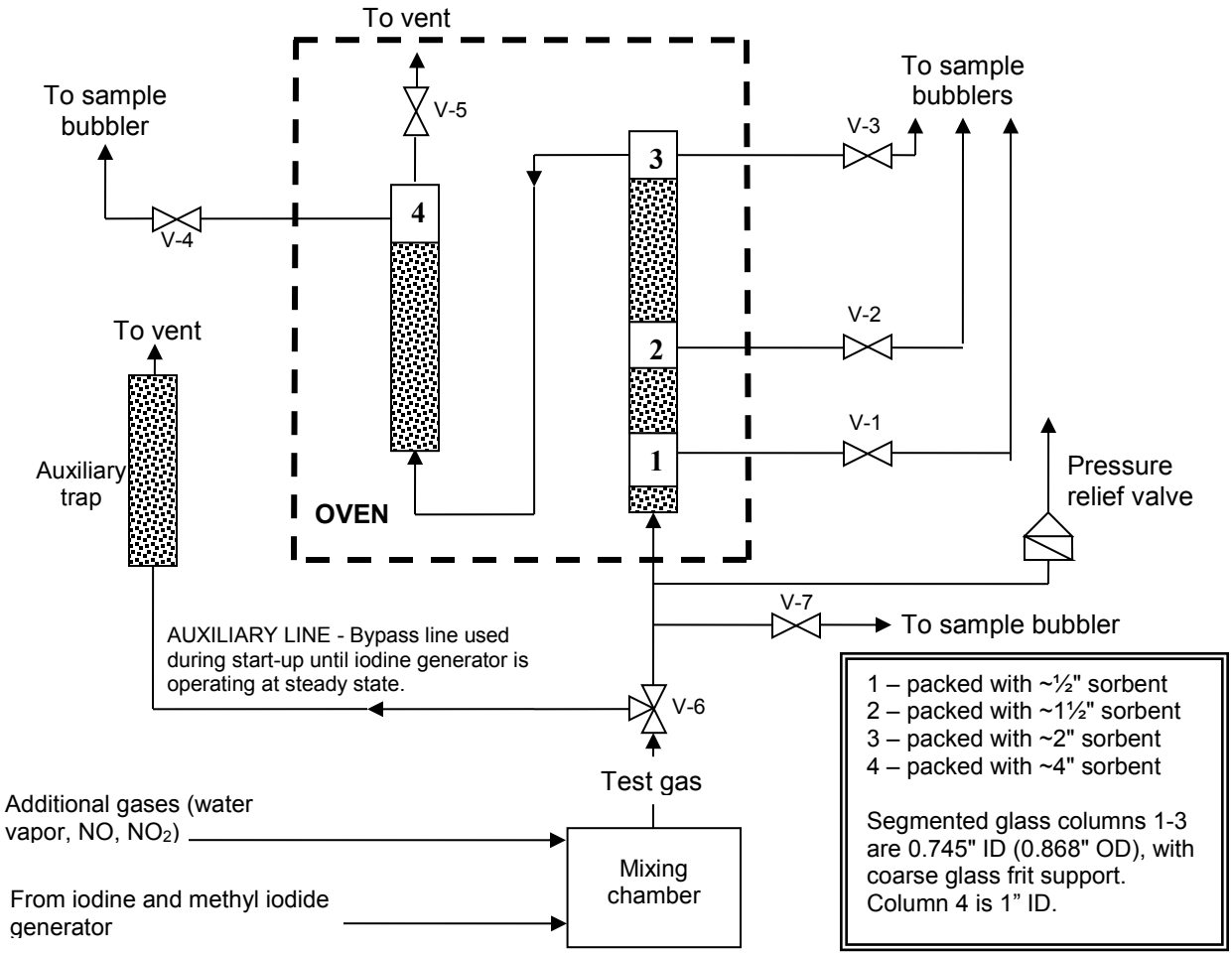

Figure 2-8. Detail of the sorbent beds.

2.4 Sample Collection and Analysis

Iodine and methyl iodide concentrations in the test gas can be measured at up to five locations in the test system – at the inlet to the sorbent bed segments, and at the outlet of each of up to four bed segments. Since the gas flowrate is essentially the same at all five sample locations, the removal efficiencies for the sorbent in all four beds can be determined by measuring the iodine and methyl iodide concentrations at these locations.

Figure 2-9. Configuration of the sorbent beds inside the temperature-controlled oven.

The iodine loadings and silver utilizations can be determined by several methods including (a) integration over time differences in the gaseous iodine concentrations for a given flowrate, (b) sorbent pre- and post-test gravimetric measurements, or (c) measurement of silver and adsorbed iodine using analytical methods such as scanning electron microscopy (SEM) energy dispersive spectroscopy (EDS) or using wet chemistry methods of sorbent digestion followed by sample analysis. Using these methods for many tests has shown that the SEM/EDS method can provide the most reliable results. The SEM/EDS method, while subject to some experimental error if not directly calibrated for silver and iodine, is not subject to (a) cumulative increasing experimental error observed in the gas analysis method, (b) experimental error in the gravimetric method due to relatively small weight changes and the potential for bias if the sorbent weight changes for other reasons such as the desorption or adsorption of other species, and (c) experimental error when portions of the sorbent are not completely digested prior to analysis.

2.4.1 Iodine Sample Collection and Analysis

Iodine measurements are made even when iodine is not included in the test gas mixture to determine if, or how much, iodine is being formed from reactions of methyl iodide.

For measuring the gaseous iodine concentration, the process gas from any of the five sample locations is passed through 25-ml "midget" impingers that contain 0.1 M NaOH for scrubbing halogen gases including I_2 and HI, if present. This technique is modeled after EPA Method 26 "Determination of Hydrogen Halide and Halogen Emissions from Stationary Sources, Non-Isokinetic Method" (40 CFR 60 Appendix A). The caustic solution scrubs the halogens by hydrolyzing halogen gases to form a proton (H^+) and hypohalous acid.

Any HI, if present, dissociates into the caustic solution, and is included with I_2 in the analysis. So this test method does not discriminate between I_2 and HI or other iodine species that are soluble in 0.1 M NaOH.

The bubbler solutions are analyzed by inductively coupled plasma mass spectrometry (ICPMS) per EPA Method 6020A (SW-846, "Test Methods for Evaluating Solid Wastes Physical/Chemical Methods," http://www.epa.gov/osw/hazard/testmethods/sw846/online/). The gaseous iodine detection limit (DL) is

about 0.08 ppb with this method. Higher–concentration samples for gas streams with 1 ppm or higher iodine concentrations are typically diluted for analysis.

2.4.2 Organic Compound Sampling and Analysis

Methyl iodide analysis using gas chromatography (GC) has evolved over time due to the corrosive nature of the typical test gas. Early testing used a Hewlett-Packard model 5890 Series II gas chromatograph (GC) installed in-line with the sample loop, thereby allowing near real-time analysis of methyl iodide [Haefner 2010]. An Rt-Q-BOND fused silica capillary column was used in the GC. The GC was equipped with an electron capture detector (ECD), which is very sensitive for measuring halogenated organic compounds. The minimum detection limit for this GC setup was about 5 ppb.

This early testing indicated that the use of the sample loop (which enables frequent and automatic sampling) and the highly sensitive ECD resulted in apparent corrosion of GC components resulting in erroneous measurements. The GC was frequently down for maintenance. Essentially all components that contacted the sample gas were eventually replaced, and the GC continued to frequently malfunction.

Beginning in FY-2013, the GC was replaced with another Hewlett Packard 5890 GC, equipped with a RTX-624, 30 m x 0.32 mm ID, 1.8 µm df column, and a flame ionization detector (FID). The sample loop was not used. This caused the sampling and analysis to be more operator time-intensive, and reduced the number of GC measurements that are practical, but reduced the amount of time that the GC components are exposed to the corrosive sample gas.

The FID is not as sensitive for methyl iodide analysis as the ECD. The methyl iodide detection limit is about 1 ppm using direct injections. When lower detection limits are desired then a solid-phase micro-extraction (SPME) syringe is used. A SPME adsorbs organic compounds onto a solid-phase sorbent in a needle, thereby concentrating the amount of analyte. The adsorbed analytes are then desorbed into the GC carrier gas at an elevated temperature.

The SPME syringe is a Supelco brand, containing 75 µm carboxen/polydimethylsiloxane fiber. The SPME and GC are calibrated together for specified adsorption and desorption times and temperatures. Using a SPME improves the methyl iodide detection limit for the FID by approximately 100x to approximately 10 ppb.

Unknown organic compounds formed by reactions of methyl iodide can appear as additional peaks on the GC-FID chromatograms. When this occurs, they can be tentatively identified using gas chromatography with mass spectroscopy (GCMS) analysis. The GCMS used for this work is a Shimadzu GC2010 with GCMS-QP2010 (with autosampler). The column is a J&W Scientific DB-1 (dimethyl polysiloxane) column, 30 m x 0.25 mm ID x 1 µm df.

3. DEEP BED METHYL IODIDE TEST RESULTS

Methyl iodide testing proceeded according to the joint methyl iodide test plan [Jubin 2012b]. One long-duration adsorption test for CH_3I on silver zeolite was completed this fiscal year. Table 3-1 summarizes the results of this test. The target CH_3I concentration in the gas stream was 50 ppm; the target NO and NO_2 concentrations were 1,000 ppm each; and no added H_2O or other gas species were included. The maximum moisture content of the gas mixture, based on specifications of the test gases, was 3 ppm (0.0003 volume %).

Table 3-1. Results of the long-duration methyl iodide test.

Run Number	CH3I-12 AgZ 50 ppm CH3I w/ NOx, no H2O	
Simulate what off-gas?	Dissolver	
Test start date	30-Jun-15	
Sorption conditions		
Temperature, deg. C	165	
Total gas flowrate, sccm	700	
Target bed inlet CH3I conc, ppmv	50	
Average measured bed inlet CH3I conc, ppmv	44.9	
Average measured bed inlet I2 conc, ppmv	0.21	
H2O conc, %	0.0003%	
NO conc., ppmv	1,000	
NO2 conc., ppmv	1,000	
Balance	air	
Gas flowrate, standard l/min	0.70	
Sorption gas velocity, m/min	4.3	
Depths of each successive orbent bed, inches	0.38, 0.88, 1.25, 2.25	
Cumulative sorbent bed depths, inches	0.38, 1.25, 2.5, 4.75	
Bed 1 out residence t, sec	0.13	
Bed 2 out cumulative residence t, sec	0.44	
Bed 3 out cumulative residence t, sec	0.89	
Bed 4 out cumulative residence t, sec	2.30	
AgZ Ag concentration from SEM/EDS, wt%	10.3%	
Iodine loadings from SEM/EDS	From SEM/ EDS	From bed weight gain
Bed 1	6.2%	5.8%
Bed 2	6.0%	5.9%
Bed 3	5.0%	3.3%
Bed 4	5.1%	2.9%
Silver utilization, %	From SEM/ EDS	From bed weight gain
Bed 1	51%	48%
Bed 2	50%	49%
Bed 3	42%	27%
Bed 4	42%	24%
Max DF before breakthrough	871	
Average conversion of CH3I to I2 (or other iodine species including HI) soluble in 0.1 N NaOH)	0.92%	
Max conversion of bed outlet CH3I to I2	99.4%	
Mass transfer zone depth, inches	>5 inches	
Organic compounds tentatively identified	Nitromethane, CH3NO2	
	Iodonaphthalene, C10H7I	
	3-Amino 1-propanol, C3H9NO	

[iodine data 16sept15.xlsx]2015 CH3I summary

This test was designed for higher NO_x concentrations, 1,000 ppm each for NO and NO_2, instead of about 800 ppm each used in prior deep-bed tests. Silver zeolite (AgZ) was the sorbent, with a presumed silver content of 9.5 wt%. This sorbent was chemically reduced to convert the silver to Ag^o and provided by Oak Ridge National Laboratory (ORNL).

The measured bed inlet CH_3I concentration averaged 44.5 ppm, reasonably close to the target of 50 ppm. The degree to which the CH_3I in the inlet gas stream was converted to other iodine species was determined by sampling the inlet gas stream for iodine species soluble in 0.1 M NaOH, such as HI or I_2. Analysis of the scrub solutions indicated an average of 0.21 ppm HI/I_2, or about 0.92% of the average measured inlet CH_3I concentration.

Figure 3-1 shows the AgZ sorbent in the sorbent beds prior to adsorption testing. The sorbent in all 4 beds consists of pellets in various shades of rust color to grey. Figure 3-2 shows the AgZ sorbent at the end of the 523 hour test. A post-test purge, intended to desorb and remove any weakly-held iodine, which was not chemisorbed on the sorbent was performed at the end of the test. The sorbent color had become uniformly lighter, with a pink or coral shade, presumably due to the normally reddish color of the adsorbed iodine. It is also possible that the species in the gas mixture have caused some coloration to fade, due to other chemical reactions. This color change is most evident in the post-test, post-purge photo in Figure 3-3, in brighter lighting outside of the oven.

Figure 3-1. AgZ sorbent in the sorbent beds prior to the test CH3I-12.

Figure 3-2. Iodine-laden AgZ sorbent in the sorbent beds at the beginning of the CH3I-12 post-test purge.

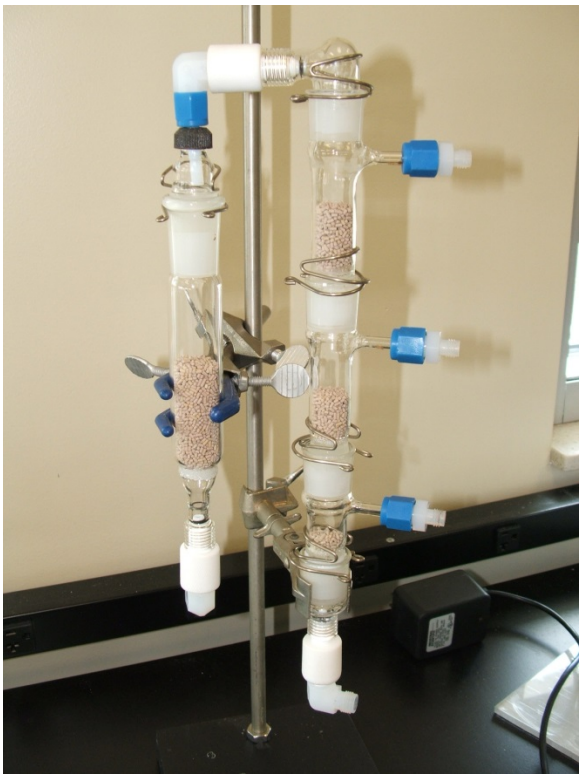

Figure 3-3. Iodine-laden AgZ sorbent in the sorbent beds following the CH3I-12 test.

3.1 Sorbent Performance in the Long-Duration Test

The decreasing trend in the sorbent DF during the test period for all four sorbent bed segments is shown in Figure 3-4. The DF was calculated by accounting for iodine in CH_3I and also iodine detected in the 0.1 M NaOH scrubbers. At the beginning of the test, the highest measured DF (at the outlet of Bed 3, 2.5 inches deep in the bed) was under 1,000 (The DF at the outlet of bed 4, almost 5 inches deep in all four beds, was somewhat lower at 648, probably due to experimental error).

These low DFs indicate that (a) the iodine adsorption mass transfer zone is over 5 inches (consistent with prior CH_3I test results [Soelberg 2014] and (b) a deeper bed would be needed in a full-scale process to reach DF levels that could be needed to meet regulatory requirements. The DF trend shows that the adsorption capability for all four beds was depleted over time, as the CH_3I was reacted to release the iodine, which was adsorbed on the sorbent. The decrease in adsorption capability was fastest for Bed 1. The adsorption ability of Bed 1 decreased to near 0 (DF approaching 1) at about 100 hours into the test. The adsorption ability of Bed 4 decreased the slowest, decreasing to a DF of around 3 by about test hour 500.

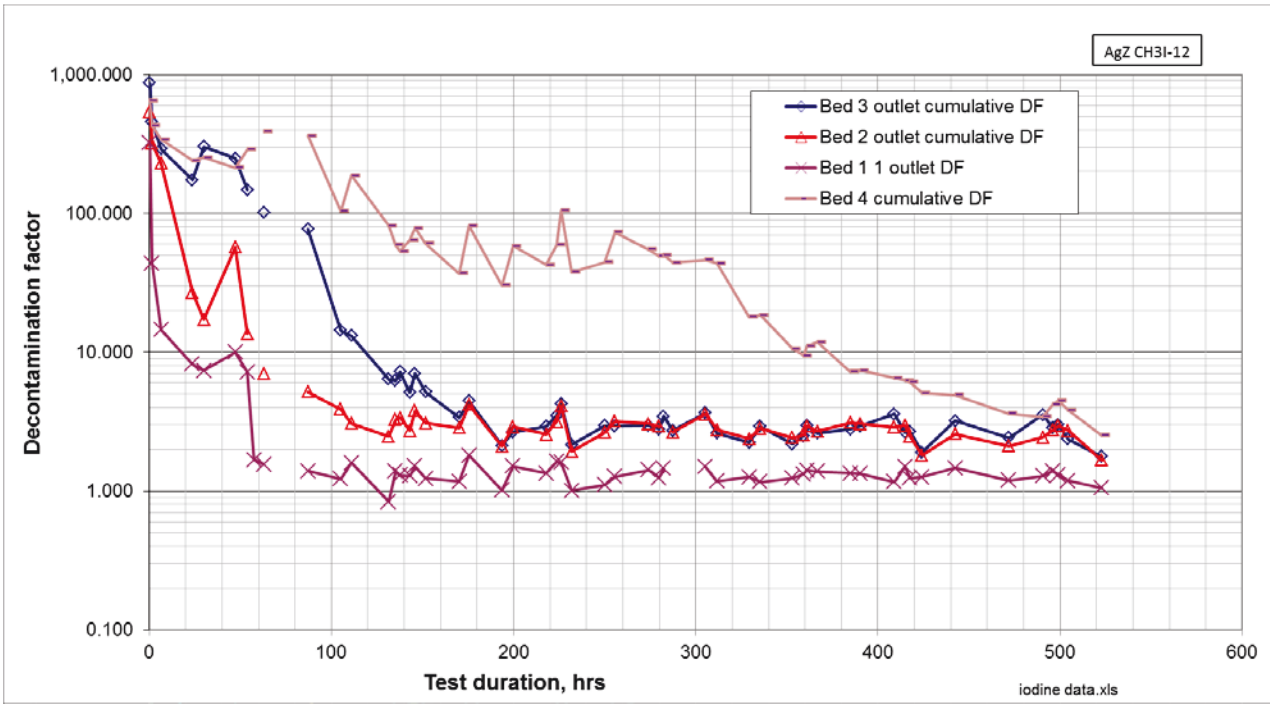

Figure 3-4. Total iodine DF trends over time.

Figure 3-5 shows the same DF data trends on a log-log scale. This figure illustrates that the decrease in Bed 1 DF over time was nearly linear, until the adsorption capacity was nearly depleted by test hour 100. The DF decrease for the other three bed segments was slower, and also nearly linear, until a faster depletion rate began which lead to near-depletion of the adsorption capacity for those beds. The change in the decrease of the adsorption capacity for Bed 2 occurred between about test hour 7 and 20, followed by faster decreases in depletion rates for Beds 3 and 4 at approximately test hours 100 and 300, respectively.

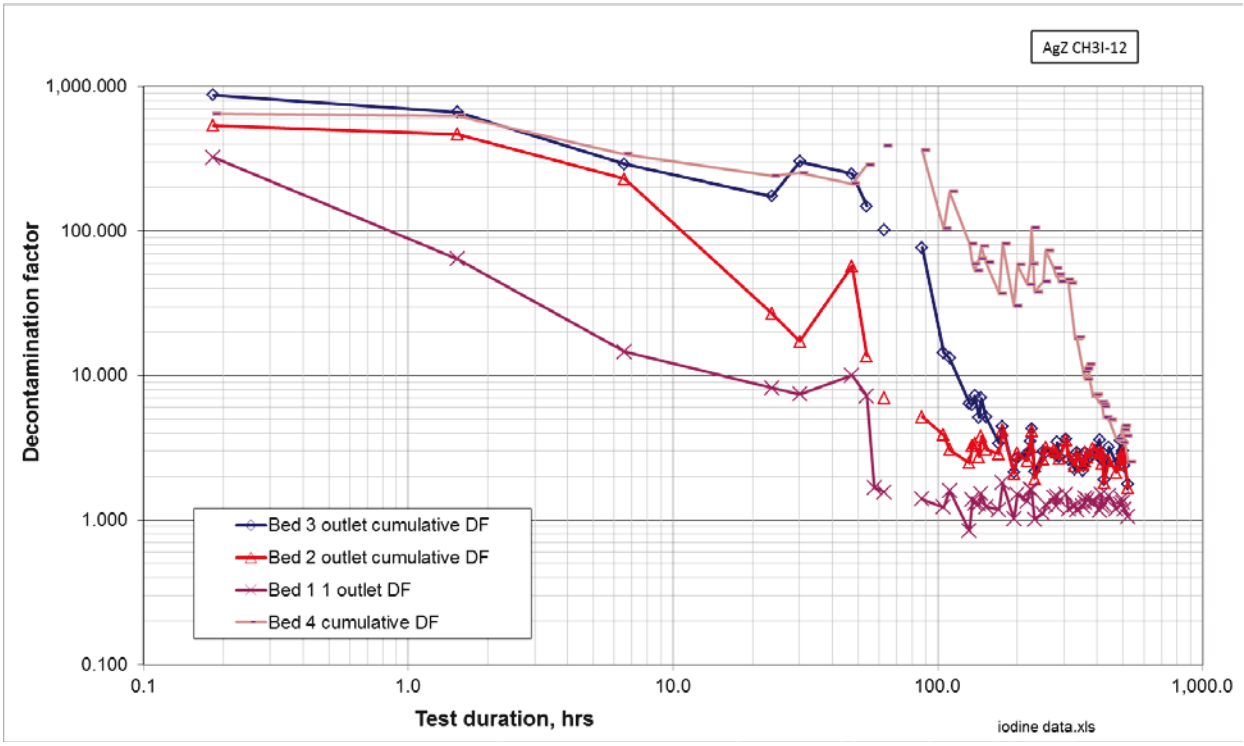

Figure 3-5.Total iodine DF trends over time on a log-log scale.

The CH_3I measurement trends are shown in Figure 3-6. This figure shows that initial bed outlet CH_3I concentrations were decreased by about three orders of magnitude for all four bed segments. The bed outlet CH_3I concentrations nearly linearly increased for all four beds (although fastest for Bed 1) until between about hours 50 and 60, when the Bed 1 outlet CH_3I concentration increased by over one order of magnitude, and about hour 400, when the bed outlet CH_3I concentrations for the other three beds increased by up to one order of magnitude.

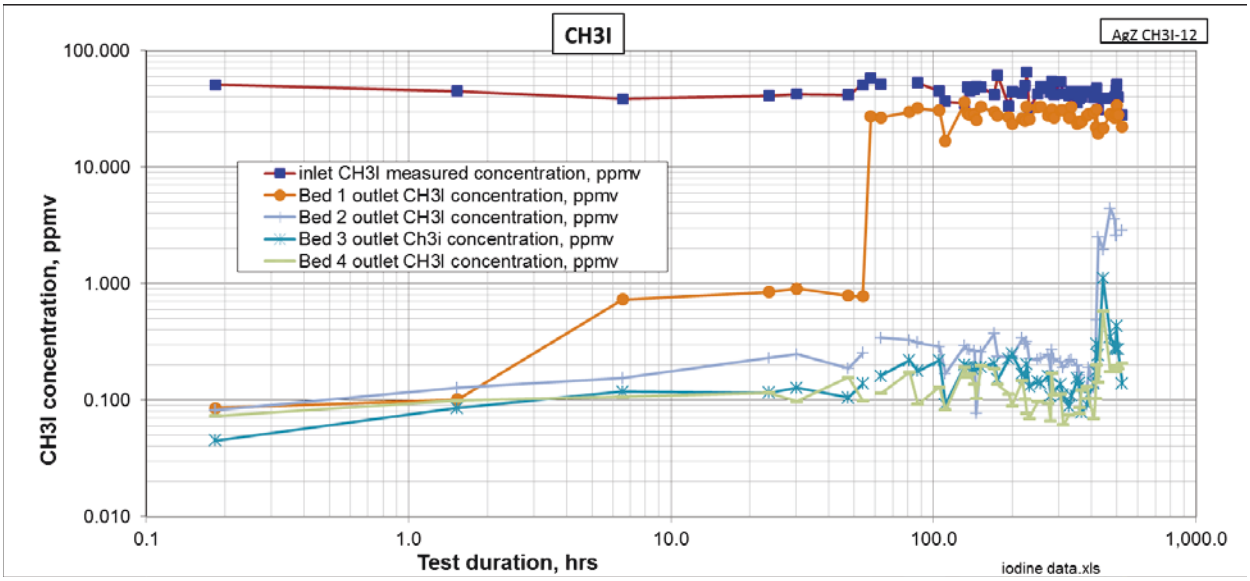

Figure 3-6. CH_3I concentration trends over time.

The increase in bed outlet CH_3I concentrations was not the only, and not the major, contributor to the decreasing DFs. Figure 3-7 shows the increase in the measured iodine species detected in the 0.1 M NaOH scrub solutions, reported as I_2. The initial Bed 1 outlet I_2 concentration was almost one order of magnitude higher than the initial bed outlet I_2 concentrations for the other bed segments. While the Bed 2-4 outlet I_2 concentrations stayed flat for about the first 8-20 hours, the Bed 1 outlet I_2 concentration had increased by about one order of magnitude by hour 20. After hour 20, the bed outlet I_2 concentrations for other beds also increased. By hour 60 the Bed 1 outlet I_2 concentration had increased by two orders of magnitude, to almost 4 ppm (about 20% of the input iodine), after which it began to decrease. This was the same time as the step-change increase in the Bed 1 outlet CH_3I concentration, when the Bed 1 adsorption capability was nearly depleted. It seems likely that when the adsorption capability of Bed 1 was nearly depleted, the increase in conversion of iodine in the CH_3I to gaseous I_2 also stopped, and in fact decreased over time so that by the end of the test, the Bed 1 outlet I_2 level decreased to about 2-3 ppm.

By test hour 200, the Bed 2 and Bed 3 outlet I_2 levels increased to about 8 ppm (about 40% of the input iodine). By the end of the test, even the Bed 4 outlet I_2 levels increased to almost the same level. The major contributor to decreasing DFs was the formation of iodine species reported as I_2, not remaining CH_3I. Figure 3-8 shows the increasing trend in total un-adsorbed iodine. Chemical reactions occur as the gas mixture passes through the sorbent bed that break up the CH_3I; and allow adsorption of iodine, until the sorbent capability is depleted, at which time the un-adsorbed iodine remains in the gas stream as iodine species that are soluble in 0.1 M NaOH.

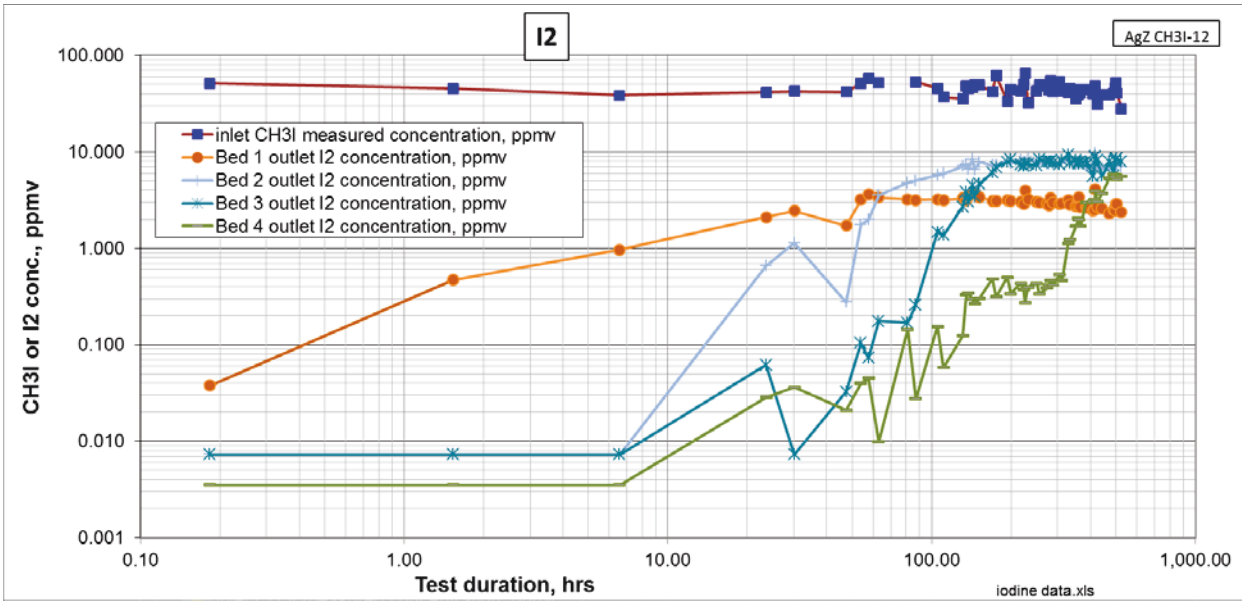

Figure 3-7. Bed segment outlet I_2 concentration trends over time.

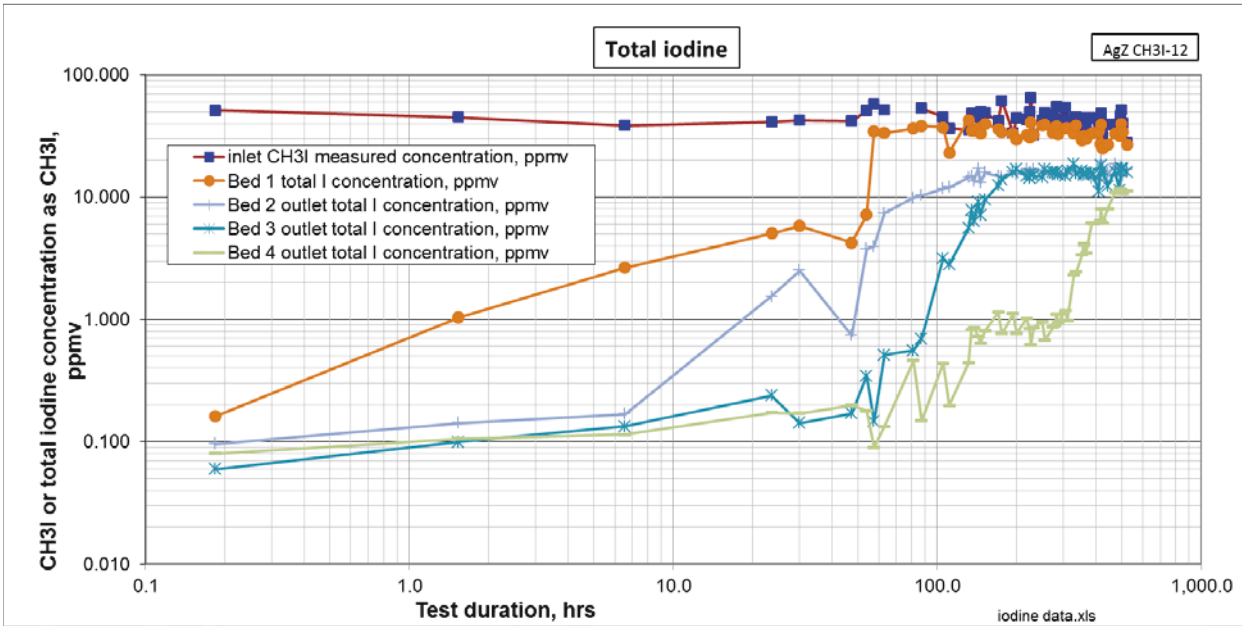

Figure 3-8. Bed segment outlet total iodine concentration trends over time.

3.2 Sorbent Capacity

Figure 3-9 shows the post-test iodine adsorption profile for the of Ag zeolite sorbent from the test. The maximum iodine loading in the first ~1.5 inches was determined using SEM/EDS measurements of the iodine in the spent sorbent to be about 6.2 wt% (6.2 g adsorbed iodine per 100 g original sorbent). The maximum silver utilization determined by SEM/EDS was about 51%.

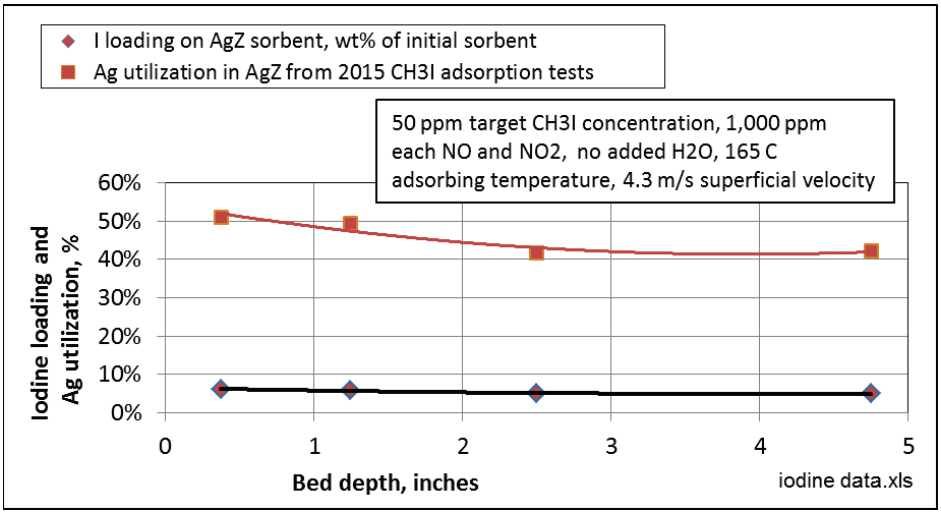

Figure 3-9. Practical iodine capacity and Ag utilization on AgZ sorbent for iodine adsorption from CH_3I in simulated DOG streams.

Results of this test are compared to other prior deep-bed iodine adsorption tests in Figure 3-10. All these tests were performed using reduced Ag zeolite. Both the capacity and Ag utilization for iodine adsorption from CH_3I were about one-half to two-thirds of the respective values for iodine adsorption from I_2 in the simulated aqueous DOG streams. This test had higher NO_x levels (2,000 ppm compared to a maximum of about 1,600 ppm for the other tests).

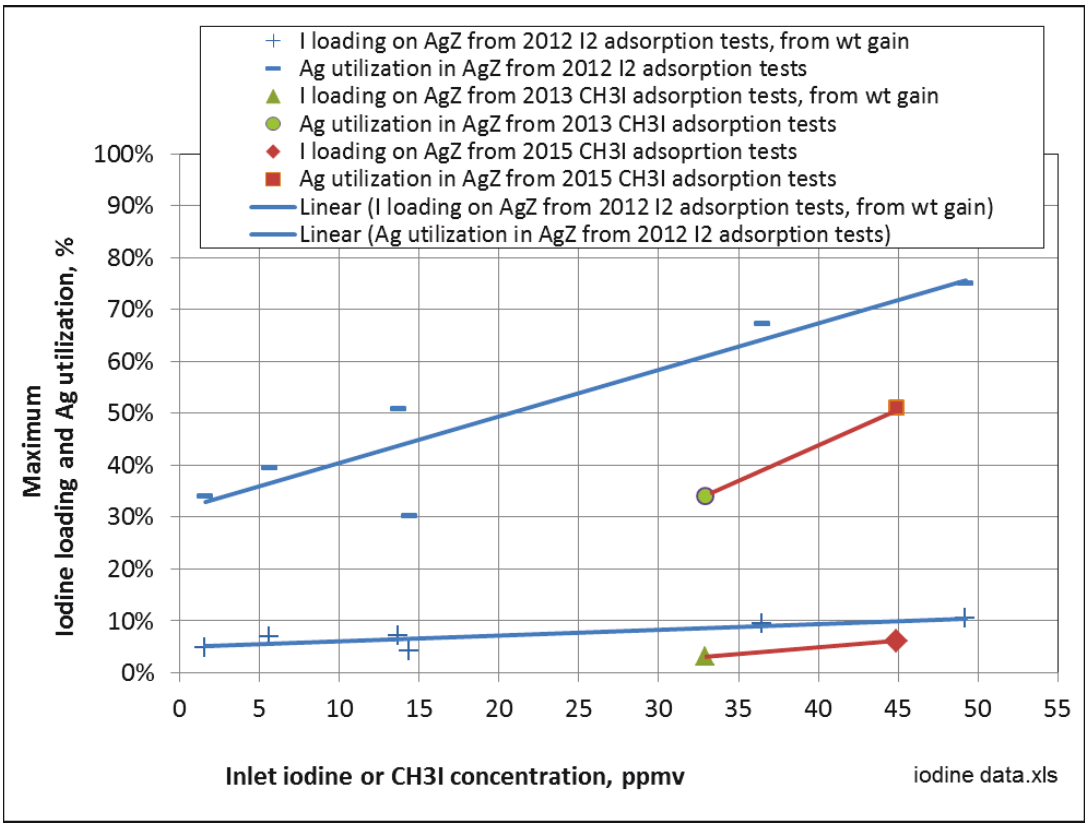

Figure 3-10. Iodine capacity for CH_3I and I_2 using reduced Ag zeolite.

3.3 Organic Species Detected in the Sorbent Bed Outlet Gas

The GC-FID chromatograms of the bed segment outlet gas showed several peaks in addition to the CH_3I peak. Peaks detected in the samples of gas from the bed outlets were periodically analyzed by GCMS in attempts to tentatively identify these organic compounds. The GCMS was not as sensitive for these organic compounds as was the GC-FID, so some peaks detected on the GC-FID chromatograms were not detected by the GCMS.

Figure 3-11 shows the GC-FID peaks for the bed inlet gas mixture. The GC-FID area count data are from the sample periods performed during the test, numbered in this figure from 2 to 54. The CH_3I peak is consistently present at a retention time of about 2.1-2.2 minutes, along with other unknown peaks with about one order of magnitude lower area counts, at retention times of about 1.35-1.45 min. The GC-FID was not calibrated for other peaks beside the methyl iodide peak, so these figures show the peak areas, not actual concentrations. If the response factor(s) for these unknowns are similar to that of CH_3I, then the concentrations of these other compounds would be about one order of magnitude lower than for the CH_3I. A few other peaks were detected with higher residence times. These were not consistent for most sample periods.

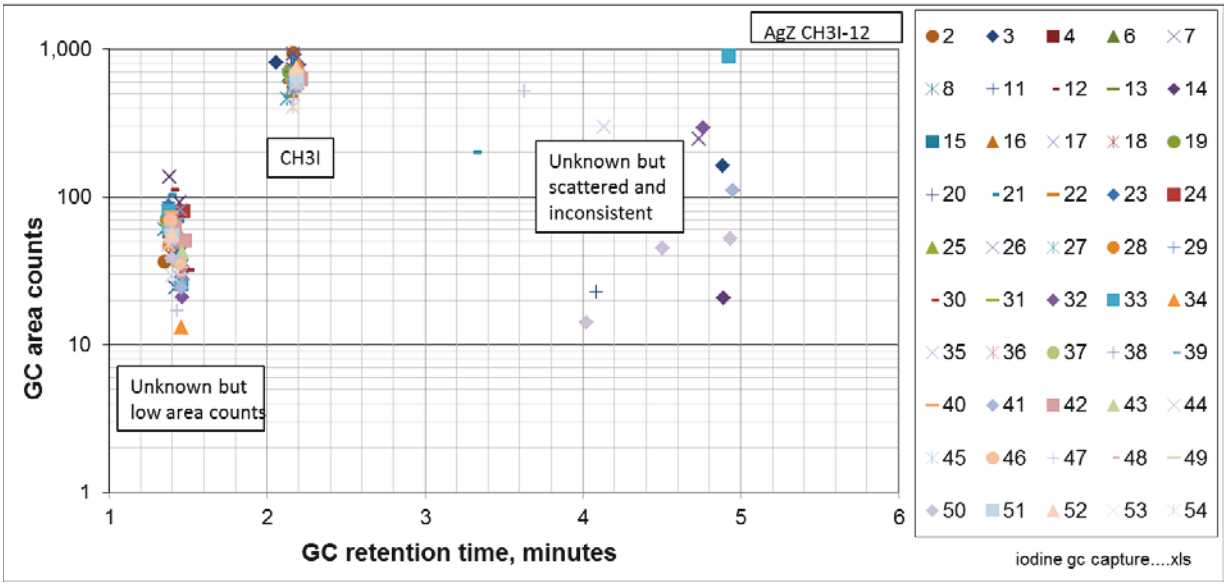

Figure 3-11. GC-FID peaks for organic compounds found in the sorbent bed inlet gas mixture.

Figure 3-12 shows the GC-FID peaks for the Bed 1 outlet gas. The CH_3I peak is consistently present at a retention time of about 2.1-2.2 minutes, along with the same other unknown peaks with about one order of magnitude lower area counts, at retention times of about 1.35-1.45 min.

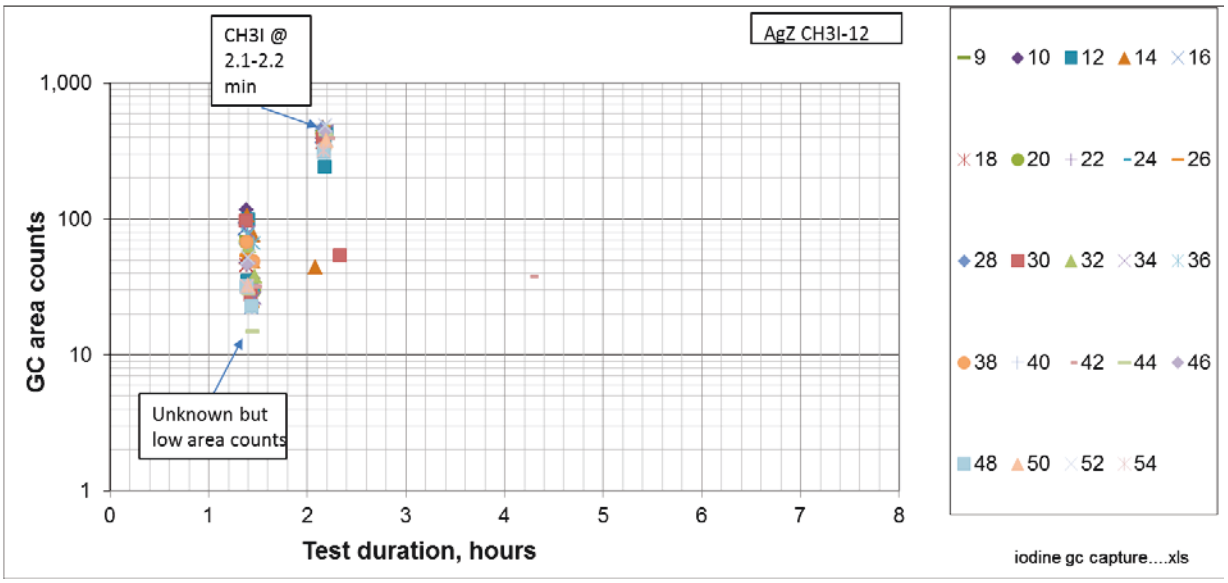

Figure 3-12. GC-FID peaks for organic compounds found in the Bed 1 outlet gas.

Figure 3-13 shows the GC-FID peaks for the Bed 4 outlet gas. The CH_3I peak is consistently present at a retention time of about 2.1-2.2 minutes, along with the same other unknown peaks with about one order of magnitude lower area counts, at retention times of about 1.35-1.45 min. Many other peaks are also consistently evident. Peaks that have been identified by GCMS include the peaks for nitromethane at retention times of about 2.3-2.4 minutes, iodonaphthalene at about 4.1 minutes, siloxane (a GC column bleed compound), and 3-amino-1-propanol at about 5.8 minutes.

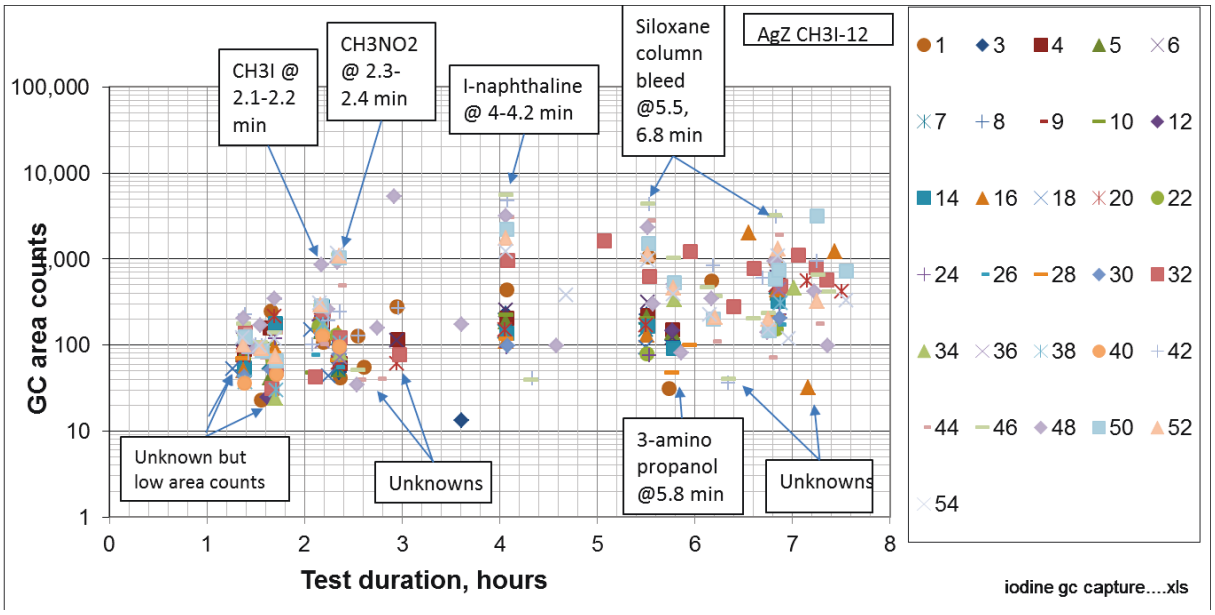

Figure 3-13. GC-FID peaks for organic compounds found in the Bed 4 outlet gas.

The theory about how the CH_3I molecule is first split up via chemical interactions with the sorbent, how the iodine is then chemisorbed, and how residual gaseous organic moieties can remain in the gas stream is provided in Nenoff 2014.

The formation of such a variety of higher molecular weight compounds as a consequence of the CH_3I adsorption process seems unlikely. These higher molecular weight compounds may be contaminants, or results of interactions of the gas stream with components in the testing, sampling, and analysis systems.

3.4 Post-Test Purging

After the test, the sorbent beds were purged to desorb any amounts of iodine that may be loosely or physisorbed. The purge results for this test are shown in Figure 3-14. This figure shows that only a small fraction of the iodine sorbed on Bed 1 (about 3%) was desorbed during the 48 hour purge period. During the purge period, the Bed 1 outlet I_2/HI level decreased by about one order of magnitude. Except for the initial CH_3I measurement, all Bed 1 outlet CH_3I measurements were below the detection limit. The detection limit values are shown in the figure.

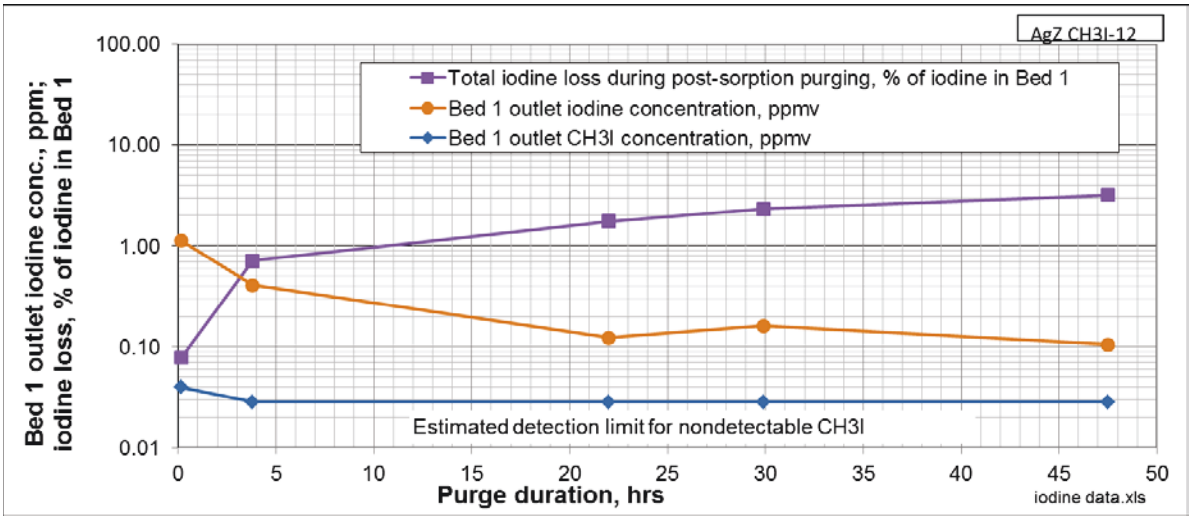

Figure 3-14. CH_3I-12 post-test sorbent purge results.

4. CONCLUSIONS AND RECOMMENDATIONS

Deep-bed methyl iodide adsorption testing has progressed according to the multi-laboratory methyl iodide adsorption test plan [Jubin 2012b]. The reaction(s) enable separation of the iodine from the organic moiety, so that the iodine can chemisorb onto the sorbent. The organic moiety can form other compounds, some of which are organic compounds that are detected and can be tentatively identified using GC-FID and GCMS.

For the first time compared to prior iodine and CH_3I tests, CH_3I initial DFs using AgZ did not exceed 1,000. The higher NO_x levels in this test might have contributed to the lower DFs. As in prior tests, the iodide mass transfer zone depth for CH_3I exceeded 5 inches, deeper than mass transfer zone depths estimated for I_2 adsorption on AgZ.

Additional deep-bed testing and analyses are recommended to (a) expand the data base for methyl iodide adsorption under various conditions specified in the methyl iodide test plan, and (b) provide more data for evaluating organic iodide reactions and reaction byproducts for different potential adsorption conditions.

5. REFERENCES

Birdwell 1991 Birdwell, J.F., 1991, Iodine and NOx Behavior in the Dissolver Off-gas and IODCX Systems in the Oak Ridge National Laboratory Integrated Equipment Test Facility, NUREG/CP—011-Vol.1, Proceedings of the 21st DOE/NRC Nuclear Air Cleaning Conference, San Diego, CA, pp. 271-298.

Bruffey 2015 Bruffey, SH, BB Spencer, DM Strachan, RT Jubin, Nick Soelberg, and BJ Riley, "A Literature Survey to Identify Potentially Problematic Volatile Iodine-Bearing Species Present in Off-Gas Streams," FCR&D-MRWFD-2015-000421, ORNL-SPR-2015/290, INL/EXT-15-35609, 30 June 2015.

Edmund 1928 Edmund, B.R. Prideaux and Herbert Lambourne, 1928, *Nitrogen*, Vol VI. Part I from J. Newton Friend, "A Text-book of Inorganic Chemistry," Charles Griffin & Co., Page 171, Figure 19.

Haefner 2010 Haefner, D. R., and T. Watson, "Summary of FY 2010 Iodine Capture Studies at the INL," INL/EXT-10-19657, August 2010.

INL 2015 INL 2015, "Gaseous Fission Product Capture Testing," Laboratory Instruction (LI) 645, Idaho National Laboratory.

Jubin 2012a R. T. Jubin, N. R. Soelberg, D. M. Strachan, and G. Ilas, 2012a, "Fuel Age Impacts on Gaseous Fission Product Capture during Separations," FCRD-SWF-2012-000089, Oak Ridge National Laboratory, 2012.

Jubin 2012b Jubin, R.T., B. B. Spencer, N. R. Soelberg, D. M. Strachan, T. M. Nenoff, 2012b, "Joint Test Plan to Identify the Gaseous By-Products of CH_3I Loading on AgZ," INL/EXT-12-27978, FCRD-SWF-2013-000070, December 26, 2012.

Jubin 2013 Jubin, R.T., D.M. Strachan, and N.R. Soelberg, "Iodine Pathways and Off-Gas Stream Characteristics for Aqueous Reprocessing Plants – A Literature Survey and Assessment," FCRD-SWF-2013-000308, ORNL/LTR-2013/383, INL/EXT-13-30119, September 15, 2013.

Law 2014 Law, J., N. Soelberg, T. Todd, J. Tripp (INL), C. Pereira, M. Williamson, W. Ebert (ANL), R. Jubin, B. Moyer (ORNL), J. Vienna, G. Lumetta, J. Crum (PNNL), T. Rudisill (SRNL), J. Bresee (DOE-NE), C. Phillips, B. Willis (EnergySolutions), P. Murray, S. Bader (AREVA), 2014, "Separation and Waste Form Campaign Full Recycle Case Study," FCRD-SWF-2013-000380, Revision 1, September 30.

Nenoff 2014 Nenoff, Tina, Mark Rodriguez, Nick Soelberg, Karen Chapman, 2014, "Silver-Mordenite for Radiologic Gas Capture from Complex Streams: Dual Catalytic CH3I Decomposition and I Confinement," Microporous and Mesoporous Materials, MICMAT6530, INL/JOU-14-31276, 9 May 2014.

Soelberg 2013 Soelberg, Nick R., Troy G. Garn, Mitchell R. Greenhalgh, Jack D. Law, Robert Jubin, Denis M. Strachan, and Praveen K. Thallapally, 2013, "Radioactive Iodine and Krypton Control for Nuclear Fuel Reprocessing Facilities," Hindawi Publishing Corporation, Science and Technology of Nuclear Installations, Volume 2013, Article ID 702496, 12 pages, http://dx.doi.org/10.1155/2013/702496.

Soelberg 2014 Soelberg, Nick and Tony Watson, "Phase 1 Methyl Iodide Deep-Bed Adsorption Tests," INL/EXT-14-32917, FCRD- SWF-2014-000271, August 22, 2014.